Inorg. Chem. **2005**, *44*, 1563–1570

Synthesis, Crystal Structure, and Properties of Multicomponent Bis(ethylenedithio)tetrathiafulvalene Charge-Transfer Salts of the $[Mo_3S_7Br_6]^{2-}$ Cluster

Rosa Llusar,*,† Sonia Triguero,† Santiago Uriel,‡ Cristian Vicent,† Eugenio Coronado,§ and Carlos J. Gomez-Garcia§

Departament de Ciències Experimentals, Universitat Jaume I, Campus de Riu Sec, P.O. Box 224, Castelló, Spain, Departamento de Química Orgánica-Química Física, Centro Politécnico Superior, Universidad de Zaragoza-ICMA, María de Luna 3, 50018, Zaragoza, Spain, and Instituto de Ciencia Molecular, Universitat de Valencia, c/Dr. Moliner No. 50, E-46100, Spain

Received August 24, 2004

A new family of bis(ethylenedithio)tetrathiafulvalene (ET) radical salts has been prepared in the presence of a triangular molybdenum sulfide cluster of formula $[Mo_3S_7Br_6]^{2-}$, which contains highly electrophilic axial sulfur atoms. A systematic change in the experimental conditions yields five different salts, namely $(ET_A)_2(ET_B)[Mo_3S_7Br_6]_2 \cdot CH_2Br_2$ (**1**), $(ET_A)(ET_B)[Mo_3S_7Br_6] \cdot 1.1CH_2Br_2$ (**2**), $(ET_A)(ET_B)(ET_C)\{[Mo_3S_7Br_6]Br\} \cdot 0.5C_2H_4Cl_2$ (**3**), (ET)((*n*-Bu_4)N)-$[Mo_3S_7Br_6]$ (**4**), and (ET)$(Ph_4P)[Mo_3S_7Br_6] \cdot 0.5CH_3CN$ (**5**), where the ET subscript denotes crystallographically independent molecules. The five compounds have been structurally characterized, and all of them crystallize in the triclinic space group $P\bar{1}$ with $Z = 2$. Lattice parameters (Å, deg) are the following: $a = 11.762(4)$, $b = 12.246(4)$, $c = 16.813(6)$, $\alpha = 107.572(9)$, $\beta = 99.133(7)$, and $\gamma = 102.856(8)$ for **1**; $a = 12.643(3)$, $b = 13.370(4)$, $c = 17.936(4)$, $\alpha = 103.884(8)$, $\beta = 95.013(7)$, and $\gamma = 114.396(6)$ for **2**; $a = 11.907(6)$, $b = 12.742(6)$, $c = 22.905(12)$, $\alpha = 90.053(15)$, $\beta = 79.063(14)$, and $\gamma = 75.802(15)$ for **3**; $a = 12.787(6)$, $b = 13.653(6)$, $c = 17.543(8)$, $\alpha = 68.398(10)$, $\beta = 69.911(12)$, and $\gamma = 62.377(10)$ for **4**; $a = 12.467(5)$, $b = 13.553(6)$, $c = 18.913(8)$, $\alpha = 85.378(11)$, $\beta = 78.576(11)$, and $\gamma = 65.858(9)$ for **5**. Structural data combined with Raman spectral analysis shows that, in salt **1**, one-third of the ET molecules, those marked as ET_B, are incorporated into the structure as ET^{2+} and two-thirds as ET^{+}. Bonds distances and Raman frequencies for donor molecules in compounds **2**–**5** suggest a 1+ charge for all ET molecules, in agreement with the stoichiometries and IR and electronic spectra of these salts. In all cases the various donor–cluster, donor–donor, and cluster–cluster interactions and those involving the solvent molecules give rise to unique arrangements of the donor molecules. A general feature of structures **1**–**5** is the presence of alternating layers of dimerized organic donor molecules (ET^{+}:ET^{+}) and of inorganic clusters, where the long axis of the donor dimers runs almost parallel to the cluster layer. There is a strong tendency of the combination {$[Mo_3S_7Br_6]$:ET} to accommodate a third bulky component. Compounds **4** and **5** incorporate $[(n\text{-}Bu_4)N]^{+}$ or $[Ph_4P]^{+}$, respectively, with no apparent interactions with the ET layers in the solid state. Compound **2** and **4** are semiconductors, while the remaining salts are insulators.

Introduction

The electron donor molecule ET [bis(ethylenedithio)-tetrathiafulvalene] has been widely used for the preparation of charge-transfer salts containing a large variety of charge-compensating anions and exhibiting a wide range of electrical properties as semiconductors, metals, and superconductors.[1−4]

* Author to whom correspondence should be addressed. E-mail: llusar@exp.uji.es. Fax: (+34)-964728066.
† Universitat Jaume I.
‡ Universidad de Zaragoza-ICMA.
§ Universitat de Valencia.

(1) Williams, J. M.; Ferraro, J. R.; Thorn, R. J.; Carlson, K. D.; Geiser, U.; Wang, H. H.; Kini, A. M.; Whangbo, M. H. *Organic Superconductors*; Prentice Hall: Upper Saddle River, NJ, 1992.
(2) Batail, P.; Boubekeur, K.; Fourmigué, M.; Gabriel, J.-C. P. *Chem. Mater.* **1998**, *10*, 3005.
(3) Ishiguro, T.; Yamaji, K.; Saito, G. *Organic Superconductors*; Springer-Verlag: New York, 1998.
(4) Day, P. *C. R. Chimie* **2003**, *6*, 301.

10.1021/ic0488379 CCC: $30.25
Published on Web 02/10/2005

These solids built from molecules give us the ability to create materials with structural complexities not found in traditional continuous lattice materials where subtle changes in the structure may lead to large differences in the properties of the molecular solid. The charge distribution, distances, and relative orientations of the donor molecules are responsible for the collective physical properties, and this may be controlled by the packing of the compensating-charge anions. Many efforts have been made aimed to increase interactions between the anion and cation sublattices and hence to increase the electronic dimensionality of the resulting molecular material. The relevance of S···S intermolecular contacts in the formation of conduction paths in organo−sulfur lattices is well documented.[1] Strategies to promote S···S interactions include the incorporation of sulfur atoms in the periphery of the compensating anions, as for example in (TTF)[Ni(dmit)$_2$]$_2$,[5] (ET)[ReO(dmit)$_2$][6] (TTF = tetrathiafulvalene, dmit = 1,3-dithia-2-thione-4,5-dithiolate), and (ET)$_4$[M(NCS)$_6$]·solvent (M = Fe, Cr),[7,8] or the use of cluster sulfide complexes, as in (ET)$_4$[Re$_6$S$_6$Cl$_8$)]·solvent.[9]

In this context the trinuclear [Mo$_3$(μ_3-S)(μ-S$_2$)$_3$Br$_6$]$^{2-}$ cluster anion, with one capping sulfur atom and three bridging disulfides, is an attractive target due to the electrophilic character of the bridging sulfur atoms located in axial positions (those out of the metal atoms plane). Other advantages of this cluster unit have to do with the easy substitution of its outer bromine atoms by a large variety of ligands and its equatorial sulfides by other chalcogenides.[10−12] In addition, a proper modification of these ligands can be accompanied by changes of interest in their third-order nonlinear optical, electrochemical, and magnetic properties.[11,13]

Systematic investigations on the preparation of charge-transfer salts show that minor changes in variables such as current applied, nature of the supporting electrolyte, or the solvent may lead to dramatic changes in the molecular structure and consequently in the collective properties of these solids.[2] In particular the transport properties of the ET charge-transfer salts containing tris(oxalato)metalate(III) anions have shown to be highly sensitive to the nature of the solvent molecules accommodated into the crystal structure. For example, the monoclinic β''-(ET)$_4$[(H$_3$O)Fe(C$_2$O$_4$)$_3$]·solvent phases are superconducting when the solvent incorporated is PhCN (T_c = 7.0 K)[14] or PhNO$_2$ (T_c = 6.2 K)[15] while a metal to insulator transition has been observed at 116 K for C$_5$H$_5$N.[16]

In some cases a third component, different from the solvent, is also introduced into the structure which through an appropriate choice may provide the molecular compound with new functionalities. Recently, several systems have been reported which show the importance of this third component in the final properties of the charge-transfer salts incorporating for instance 18-crown-6 ether molecules which led to the first charge-transfer salts containing proton channels.[4,17] Iodine-containing neutral molecules act as a "template" within the family of ET charge-transfer salts with Br$^-$, Cl$^-$, I$^-$, and AuBr$_2^-$ as compensating anions to give a wide variety of solid phases with semiconductor and metallic behavior.[18,19]

In this work, we report on the electrochemical synthesis of a new family of charge-transfer salts derived from the cluster unit [Mo$_3$S$_7$Br$_6$]$^{2-}$. The crystal structures of (ET)$_3$-[Mo$_3$S$_7$Br$_6$]$_2$·CH$_2$Br$_2$ (**1**), (ET)$_2$[Mo$_3$S$_7$Br$_6$]·1.1CH$_2$Br$_2$ (**2**), (ET)$_3${[Mo$_3$S$_7$Br$_6$]Br}·0.5C$_2$H$_4$Cl$_2$ (**3**), (ET)((*n*-Bu$_4$)N)[Mo$_3$S$_7$-Br$_6$] (**4**), and (ET)(Ph$_4$P)[Mo$_3$S$_7$Br$_6$]·0.5CH$_3$CN (**5**) have been determined. All complexes except **1** show the donor ET molecule in a +1 oxidation state. In complex **1**, oxidations states +1 and +2 coexist despite that no external oxidation reagent has been used in its preparation.[20] Although this fact does not necessarily imply the existence of promising conductive properties, the study of their transport properties in conjunction with those of complexes **2**−**5** will provide a better understanding of the relation between the molecular and electronic structures in these materials. Interestingly, compounds **4** and **5** show the presence of bulky cations together with the donor molecule leading to rare ternary phases that have only been previously observed in the following salts: (TTF)$_2$(Et$_4$N)[Nb$_6$Cl$_{18}$]CH$_3$CN; κ-(ET)$_4$-(Et$_4$N)M(CN)$_6$·3H$_2$O (M = Fe, Co); (TTF)$_6$(Et$_4$N)(H)-[XM$_{12}$O$_{40}$] (M = W, Mo; X = P, Si); κ-(BET)$_4$(Et$_4$N)$_2$Fe-(CN)$_6$.[21−24] These results prove the versatility of the

(5) Canadell, E.; Rachidi, I. E. I.; Ravy, S.; Pouget, J. P.; Brossard, L.; Legros, J. P. *J. Phys. (Paris)* **1989**, *50*, 2967.
(6) Domercq, B.; Fourmigue, M. *Eur. J. Inorg. Chem.* **2001**, 1625.
(7) Turner, S. S.; Day, P.; Gelbrich, M. B.; Hursthouse, M. *J. Solid State Commun.* **2001**, *159*, 385.
(8) Thetiot, F.; Berezovsky, F.; Triki, S.; Pala, J. S.; Gomez-Garcia, C. J.; Hajem, A. A.; Bouguessa, S.; Fabre, J. M. *C. R. Chim.* **2003**, *6*, 291.
(9) Pénicaud, A.; Boubekeur, K.; Batail, P.; Canadell, E.; Auban-Seinzer, P.; Jèrome, D. *J. Am. Chem. Soc.* **1993**, *115*, 4101.
(10) Bereau, V.; Pernin, C. G.; Ibers, J. A. *Inorg. Chem.* **2000**, *39*, 854.
(11) Garriga, J. M.; Llusar, R.; Uriel, S.; Vicent, C.; Usher, A. J.; Lucas, N. T.; Humphrey, M. G.; Samoc, M. *J. Chem. Soc., Dalton Trans.* **2003**, 4546.
(12) Fedin, V. P.; Sokolov, M. N.; Fedorov, V. Y.; Yufit, D. S.; Struchkov, Y. T. *Inorg. Chim. Acta* **1991**, *179*, 35.
(13) Llusar, R.; Uriel, S.; Vicent, C.; Coronado, E.; Gomez-Garcia, C. J.; Clemente-Juan, J. M.; Braida, B.; Canadell, E. *J. Am. Chem. Soc.* **2004**, *126*, 12076.
(14) Kurmoo, M.; Graham, A. W.; Day, P.; Coles, S. J.; Hursthouse, M. B.; Caulfield, J. L.; Singleton, J.; Pratt, F. L.; Hayes, W.; Ducasse, L.; Guionneau, P. *J. Am. Chem. Soc.* **1995**, *117*, 12209.
(15) Rashid, S.; Turner, S. S.; Day, P.; Howard, J. A. K.; Guionneau, P.; McInnes, E. J. L.; Mabbs, F. E.; Clark, R. J. H.; Firth, S.; Biggs, T. *J. Mater. Chem.* **2001**, *11*, 2095.
(16) Turner, S. S.; Day, P.; Malik, K. M. A.; Hursthouse, M. B.; Teat, S. J.; McLean, E. J.; Martin, L.; French, S. A. *Inorg. Chem.* **1999**, *38*, 3543.
(17) Rashid, S.; Turner, S. T.; Day, P.; Light, M. E.; Hursthouse, M. B.; Firth, S.; Clark, R. J. H. *J. Chem. Soc., Chem. Commun.* **2001**, 1462.
(18) Yamamoto, H. M.; Yamaura, J. I.; Kato, R. *J. Am. Chem. Soc.* **1998**, *120*, 5905.
(19) Yamamoto, H. M.; Maeda, R.; Yamamura, J.; Kato, R. *Synth. Met.* **2001**, *120*, 781.
(20) Chou, L.-K.; Quijada, M. A.; Clevenger, M. B.; de Oliveira, G. F.; Abboud, K. A.; Tanner, D. B.; Talham, D. R. *Chem. Mater.* **1995**, *7*, 530.
(21) Pénicaud, A.; Batail, P.; Davidson, P.; Levelut, A.-M.; Coulon, C.; Perrin, C. *Chem. Mater.* **1990**, *2*, 117.
(22) Le Maguerès, P.; Ouahab, L.; Conan, N.; Gomez-Garcia, C. J.; Delhaès, P.; Even, J.; Bertault, M. *Solid State Commun.* **1996**, *97*, 27.
(23) Ouhalab, L.; Bencharif, M.; Mhanni, A.; Pelloquin, D.; Halet, J. F.; Peña, O.; Garrigou-Lagrange, C.; Amiell, J.; Delhaès, P. *Chem. Mater.* **1992**, *4*, 666.
(24) Clemente-Leon, M.; Coronado, E.; Galan-Mascaros, J. R.; Gimenez-Sainz, C.; Gomez-Garcia, C. J.; Ribera, E.; Vidal-Gancedo, J.; Rovira, C.; Canadell, E.; Laukhin, V. *Inorg. Chem.* **2001**, *40*, 3526.

Table 1. Experimental Conditions for the Preparation of Salts **1**−**5**

reactants	reactant amt (mg)	solvent	products
$((n\text{-}Bu_4)N)_2[Mo_3S_7Br_6]$	10	CH_3CN/CH_2Br_2 (5:1)	$(ET)_3[Mo_3S_7Br_6]_2\cdot CH_2Br_2$[a] (**1**) (major product)
$((n\text{-}Bu_4)N)Br$	20		$(ET)_2[Mo_3S_7Br_6]\cdot 1.1CH_2Br_2$[b] (**2**)
$[((n\text{-}Bu_4)N)_2[Mo_3S_7Br_6]$	20	CH_3CN/CH_2Br_2 (5:1)	$(ET)_3[Mo_3S_7Br_6]_2\cdot CH_2Br_2$[a] (**1**)
$((n\text{-}Bu_4)N)Br$	20		$(ET)_2[Mo_3S_7Br_6]\cdot 1.1CH_2Br_2$[b] (**2**) (major product)
$((n\text{-}Bu_4)N)_2[Mo_3S_7Br_6]$	10	CH_3CN/DCE (5:1)	$(ET)_3\{[Mo_3S_7Br_6]Br\}\cdot 0.5DCE$[a] (**3**) (major product)
$((n\text{-}Bu_4)N)Br$	20		$(ET)((n\text{-}Bu_4)N)[Mo_3S_7Br_6]$[b] (**4**)
$((n\text{-}Bu_4)N)_2[Mo_3S_7Br_6]$	20	CH_3CN/DCE (5:1)	$(ET)_3\{[Mo_3S_7Br_6]Br\}\cdot 0.5DCE$[a] (**3**)
$((n\text{-}Bu_4)N)Br$	20		$(ET)((n\text{-}Bu_4)N)[Mo_3S_7Br_6]$[b] (**4**) (major product)
$((n\text{-}Bu_4)N)_2[Mo_3S_7Br_6]$	20	CH_3CN/DCE (5:1)	$(ET)(Ph_4P)[Mo_3S_7Br_6]\cdot 0.5CH_3CN$[a,b] (**5**)
$(Ph_4P)Br$	20		

[a] Crystals harvested from the anode. [b] Crystals harvested from the walls.

Table 2. Crystallographic Data for $(ET)_3[Mo_3S_7Br_6]_2\cdot CH_2Br_2$ (**1**), $(ET)_2[Mo_3S_7Br_6]\cdot 1.1CH_2Br_2$ (**2**), $(ET)_3\{[Mo_3S_7Br_6]Br\}\cdot 0.5DCE$ (**3**), $(ET)((n\text{-}Bu_4)N)[Mo_3S_7Br_6]$ (**4**), and $(ET)(Ph_4P)[Mo_3S_7Br_6]\cdot 0.5CH_3CN$ (**5**)

param	1	2	3	4	5
empirical formula	$C_{15.50}H_{13}Br_7Mo_3S_{19}$	$C_{21.10}H_{18.20}Br_{8.20}Mo_3S_{23}$	$C_{31}H_{26}Br_7ClMo_3S_{31}$	$C_{26}H_{44}Br_6Mo_3NS_{15}$	$C_{35}H_{29.50}Br_6Mo_3N_{0.50}PS_{15}$
fw	1655.59	1952.22	2275.02	1618.80	1736.24
cryst system	triclinic	triclinic	triclinic	triclinic	triclinic
a, Å	11.762(4)	12.643(3)	11.907(6)	12.787(6)	12.467(5)
b, Å	12.246(4)	13.370(4)	12.742(6)	13.653(6)	13.553(6)
c, Å	16.813(6)	17.936(4)	22.905(12)	17.543(8)	18.193(8)
α, deg	107.572(9)	103.884(8)	90.053(15)	68.398(10)	85.378(11)
β, deg	99.133(7)	95.013(7)	79.063(14)	69.911(12)	78.576(11)
γ, deg	102.856(8)	114.396(6)	75.802(15)	62.377(10)	65.858(9)
V, Å^3	2183.4(14)	2620.1(11)	3304(3)	2466.9(19)	2750(2)
T, K	293(2)	293(2)	293(2)	293(2)	293(2)
space group	$P\bar{1}$	$P\bar{1}$	$P\bar{1}$	$P\bar{1}$	$P\bar{1}$
Z	2	2	2	2	2
μ(Mo Kα), mm^{-1}	8.179	7.900	5.845	6.269	5.660
reflcns collcd	12 562	15 097	15 747	14 231	15 352
ϕ range for data collcn, deg	1.31−25.00	1.20−25.00	0.91−25.00	1.28−25.00	1.14−25.00
unique reflcns/R_{int}	7686/0.0705	9201/0.0940	11 251/0.1151	8663/0.1137	9586/0.1135
goodness-of-fit on F^2	0.926	0.987	1.022	0.954	1.124
R1[a]/wR2[b]	0.0622/0.1387	0.0771/0.1745	0.0883/0.1901	0.0777/0.1774	0.0996/0.2238
R1[a]/wR2[b] (all data)	0.1351/0.1654	0.1725/0.2234	0.2444/0.2672	0.1986/0.2493	0.1912/0.2805
resid ρ, e Å^{-3}	1.446 and −0.942	1.809 and −2.180	1.684 and −1.137	1.568 and −1.174	1.819 and −2.520

[a] $R1 = \sum||F_o| - |F_c||/\sum F_o$. [b] $wR^2 = [\sum[w(F_o^2 - F_c^2)^2]/\sum[w(F_o^2)^2]]^{1/2}$.

combination {$[Mo_3S_7Br_6]$:ET} to yield new charge-transfer salts which accommodate a third bulky component.

Experimental Section

Synthesis of Starting Materials. Compound $((n\text{-}Bu_4)N)_2[Mo_3S_7Br_6]$ was prepared as described by Fedin et al.[25] by employing $[(n\text{-}Bu_4)N]^+$ as countercation and recrystallized twice from acetonitrile/diethyl ether. Commercial chemicals, ET from Fluka and $((n\text{-}Bu_4)N)Br$ and $(Ph_4P)Br$ from Strem, and solvents, 1,2-dichloroethane (DCE) and CH_2Br_2 from Aldrich, were used as received. CH_3CN was dried over CaH_2, filtered on basic Al_2O_3, and degassed before use.

Electrocrystallization. Crystal growth took place in H-shaped electrocrystallization cells with a platinum electrode in each arm separated by a glass frit in the "H" cross piece. The $((n\text{-}Bu_4)N)_2[Mo_3S_7Br_6]$ cluster (10−20 mg) and the supporting electrolyte $((n\text{-}Bu_4)N)Br$ or $(Ph_4P)Br$ (20 mg) were placed in both compartments, and the cell was filled with a mixture of CH_3CN with a second solvent, CH_2Br_2 or DCE. ET (7 mg) was placed in the anode compartment, and a constant current of 0.4 μA was applied across the cell at a temperature of 293 K. In all cases, after 3 days, crystallization of brown plate crystals began on the electrode surface and on the walls of the cell. Table 1 shows the details of the experimental conditions employed for the preparation of salts **1**−**5**. In the absence of a second solvent, CH_2Br_2 or DCE, brown noncrystalline solids are formed instead of crystalline materials. Lower concentrations of the cluster dianion result in a preferential formation of compounds **1** and **3**.

X-ray Crystallographic Study. The crystals are air stable and were mounted on the tip of a glass fiber with the use of epoxy cement. X-ray diffraction experiments were carried out on a Bruker SMART CCD diffractometer using Mo Kα radiation ($\lambda = 0.710\ 73$ Å) at room temperature. The data were collected with a frame width of 0.3° in ω and a counting time of 25 s/frame for compounds **1**−**4** and 35 s/frame for **5** at a crystal to detector distance of 4 cm. The diffraction frames were integrated using the SAINT package and corrected for absorption with SADABS.[26,27]

The structures were solved by direct methods and refined by the full-matrix method on the basis of F^2 using the SHELXTL software package.[28] Relevant crystallographic data and structure determination parameters for the five salts are given in Table 2. In compounds **1** and **2** all cluster and ET atoms were refined anisotropically. Half a molecule of CH_2Br_2 was found in compound **1** which was refined isotropically while compound **2** showed two independent CH_2Br_2 molecules which were refined isotropically as rigid groups with an occupancy of 0.6 and 0.5. In compound **3**

(25) Fedin, V. P.; Sokolov, M. N.; Mironov, Y. V.; Kolesov, B. A.; Tkachev, S. V.; Fedorov, V. Y. *Inorg. Chim. Acta* **1990**, *167*, 39.

(26) *SAINT*, 5.0 ed.; Bruker Analytical X-ray Systems: Madison, WI, 1996.

(27) Sheldrick, G. M. *SADABS empirical absorption program*; University of Göttingen: Göttingen, Germany, 1996.

(28) Sheldrick, G. M. *SHELXTL*, 5.1 ed.; Bruker Analytical X-ray Systems: Madison, WI, 1997.

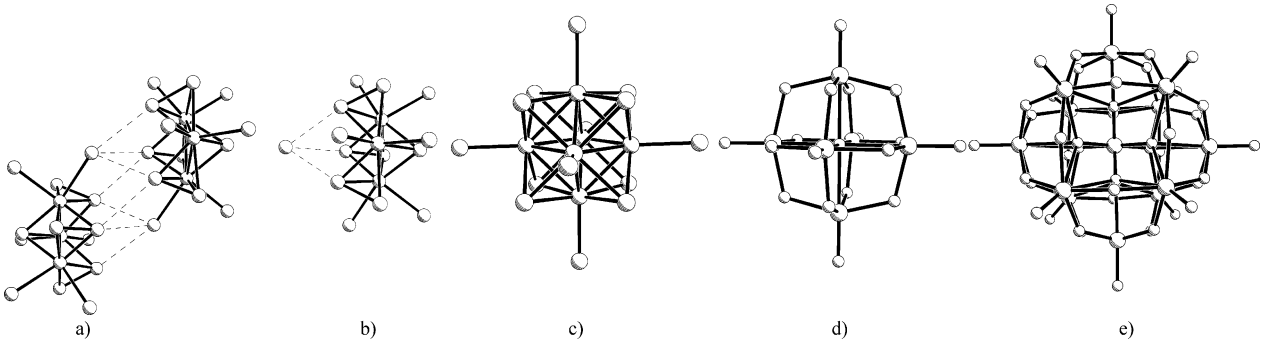

Figure 1. Comparison of the size and shape of the inorganic cluster motifs used in this work, (a) $\{[Mo_3S_7Br_6]_2\}^{4-}$ and (b) $\{[Mo_3S_7Br_6]Br\}^{3-}$, together with those of other related cluster anions draw at approximately the same scale, (c) $[Re_6S_6Cl_8]^{2-}$,[9] (d) $[Mo_6O_{19}]^{2-}$,[43] and (e) $[SiW_{12}O_{40}]^{4-}$.[32]

the ET carbon atoms and solvent were refined isotropically. In compounds **4** and **5**, all cluster and organic donor atoms were refined anisotropically while $[(n\text{-}Bu_4)N]^+$ and $[Ph_4P]^+$ atoms as well as the solvent atoms had to be refined isotropically. The $[(n\text{-}Bu_4)N]^+$ cation in **4** appeared seriously disordered and was modeled as a rigid group with partial occupancies in two nearby positions. In compounds **3** and **5**, solvent molecules (1,2-dichloroethane for **3** and acetonitrile for **5**) were refined as partially occupied (50%) under rigid conditions. In all compounds except **4**, hydrogen atoms belonging to the ET molecules and $[Ph_4P]^+$ cations were generated geometrically, assigned isotropic thermal parameters, and allowed to ride on their respective parent carbon atoms. Hydrogen atoms of the solvent molecules and the $[(n\text{-}Bu_4)N]^+$ cation were not included in the refinement.

Physical Measurements. IR spectra were recorded on a Perkin-Elmer System 2000 FT-IR using KBr pellets. Raman spectra were recorded on a Perkin-Elmer System 2000 NIR-FT instrument equipped with a diode-pumped Nd:YAG laser PSU. The position of the sample was manually adjusted, for each case, to obtain the maximum intensity for a laser power of 350 mW. NIR−vis spectra were recorded in the 4000−25000 cm^{-1} range using a VARIAN UV/vis spectrophotometer (model CARY 500 SCAN). DC conductivity measurements over the range 2−300 K were performed with the standard four contacts method on single crystals with a commercial equipment (Quantum Design PPMS-9). Contacts to the samples were made by platinum wires (25 μm diameter) attached by graphite paste to the samples. The cooling and warming rate was 1 K/min, and the intensity of the applied dc current was 1 μA.

Results and Discussion

Synthesis. The trinuclear cluster $[Mo_3S_7Br_6]^{2-}$ has been extensively used as starting material in the preparation of numerous triangular compounds due to its potential of being chemically modified by reduction of its disulfide bridges or by substitution of its bromine atoms to afford complexes with Mo_3S_4 and Mo_3S_7 moieties, respectively.[25,29] In contrast, the use of this anion for the preparation of hybrid charge-transfer salts remains still unexplored despite the growing interest in employing transition metal anions of higher complexity with a large variety of shapes, charges, and electronic structures. This is illustrated with the introduction of anions such as $[FeCl_4]^-$,[30] $[Nb_6Cl_8]^{3-}$,[21] and polyoxometalates[31,32] or the family of the isostructural and isosteric cluster anions $[Re_6Q_5Cl_9]^-$ and $[Re_6Q_6Cl_8]^{2-}$ (Q = S, Se).[9,33,34]

Two of the key factors determining the molecular and electronic structures of the final molecular solid are the size and charge carried out by the anion. These are represented in Figure 1 together with those of other anions commonly used for the preparation of hybrid charge-transfer salts.

The absence of redox activity upon oxidation in the $[Mo_3S_7Br_6]^{2-}$ cluster precludes any tuning of the band filling of the cation sublattice through anion oxidation. However this anion is a promising candidate for the formation of supramolecular aggregates due to the capability of its electrophilic axial sulfur atoms and its electronegative bromine atoms to interact with the organic sublattice either with the sulfur atoms or the hydrogen atoms from the ethylene groups, thus increasing the electronic dimensionality of the material.

Electrooxidation of ET in the presence of $((n\text{-}Bu_4)N)_2[Mo_3S_7Br_6]$ and an excess of $((n\text{-}Bu_4)N)Br$ as supporting electrolyte affords high-quality crystals when the mixtures CH_3CN/CH_2Br_2 (5:1) and CH_3CN/DCE (5:1) are used as solvent. The incorporation of solvent molecules of CH_2Br_2 or DCE is a determining factor to obtain a good packing in these molecular structures. Experiments done in CH_3CN/CH_2Br_2 afford two different phases; crystals with stoichiometry $(ET)_3[Mo_3S_7Br_6]_2\cdot CH_2Br_2$ (**1**) are harvested from the anode while a less oxidized phase, namely $(ET)_2[Mo_3S_7Br_6]\cdot 1.1CH_2Br_2$ (**2**), is collected from the cell walls. The crystal structures of compounds **1** and **2** are closely related as we will see in the next subsection. Substitution of CH_2Br_2 by DCE provides also two different phases; one formulated as $(ET)_3\{[Mo_3S_7Br_6]Br\}\cdot 0.5DCE$ (**3**) grows at the anode, while the crystalline phase $(ET)((n\text{-}Bu_4)N)[Mo_3S_7Br_6]$ (**4**) precipitates at the bottom of the cell. In contrast with phase **1** grown in CH_2Br_2, compounds **2**−**4** have all ET molecules in the same +1 oxidation state as we will discuss in the next section from the bond distance and spectroscopic analysis. Solvent molecules in compounds **1**−**3** are loosely packed as reflected

(29) Meienberger, M. D.; Hegetschweiler, K.; Ruegger, H.; Gramlich, V. *Inorg. Chim. Acta* **1993**, *213*, 157.
(30) Yu, H.; Zhang, B.; Zhu, D. *J. Mater. Chem.* **1998**, *8*, 77.
(31) Coronado, E.; Gomez-Garcia, C. J. *Chem. Rev.* **1998**, *98*, 273.
(32) Gomez-Garcia, C. J.; Gimenez-Saiz, C.; Triki, S.; Coronado, E.; Le Magueres, P.; Ouahab, L.; Ducasse, L.; Sourisseau, C.; Delhaes, P. *Inorg. Chem.* **1995**, *34*, 4139.
(33) Boubekeour, K.; Lenoir, C.; Batail, P.; Carlier, R.; Tallec, A.; Le-Paillard, M. P.; Lorcy, D.; Robert, A. *Angew. Chem, Int. Ed. Engl.* **1994**, *33*, 1379.
(34) Gabriel, J. C. P.; Boubekeur, K.; Uriel, S.; Batail, P. *Chem. Rev.* **2001**, *101*, 2037.

by the crystallographic disorder precluding a reliable analysis of the role of this component in the packing.

The third component in phase **4**, namely the $[(n\text{-}Bu_4)N]^+$ cation, comes from the supporting electrolyte, and it is well-defined crystallographically. We have investigated the possibility of extending this finding to other cations of similar topology such as $[Ph_4P]^+$. Electrocrystallization experiments done in mixtures CH_3CN/DCE indicate that such replacement is possible, and compound $(ET)(Ph_4P)[Mo_3S_7Br_6]\cdot 0.5CH_3CN$ (**5**) was harvested from both anode and the cell walls. The presence of tetrabutylammonium or tetraphenylphosphonium cations in the lattice of compounds **4** and **5** suggests a strong tendency of the combination $\{[Mo_3S_7Br_6]:ET\}$ to accommodate a third bulky component which, unlike the solvent, is crystallographically well-defined, thus making their structural role analyses more reliable.

A common feature of all the compounds obtained in this work is the presence of high oxidation states in the donor ET molecules. Although the vast majority of conducting and superconducting charge-transfer salts reported up to date have a nonintegral oxidation state between +0.5 and +1, solids with oxidation states ranging between +1 and +2 can also be conductors with potential interesting properties, distinct from those observed for the most common charge-transfer salts, due to the differences in the band-filling degree.[35]

Crystal Structures. The crystal structures of salts **1**, **2**, **4**, and **5** contain discrete supramolecular $\{[Mo_3S_7Br_6]_2\}$ bicluster units formed by interaction between the three axial sulfur atoms of one trimer with the bromine ligands of its neighbor trinuclear cluster (S···Br contacts range between 3.27 and 3.48 Å) to give tetraanions with an ellipsoidal shape and 4− charge (see Figure 1a). Interatomic distances within the cluster are statistically identical with those observed for the $(Et_4N)_2[Mo_3S_7Br_6]$ precursor.[10] In compound **3** the three axial sulfur atoms interact with one isolated bromine ion to produce trianionic $\{[Mo_3S_7Br_6]Br\}$ aggregates (see Figure 1b). Inter- and intramolecular distances within this aggregate are similar to those found in the reported oxalate derivative of formula $((n\text{-}Bu_4)N)_3\{[Mo_3S_7(C_2O_4)_3]Br\}$ which also contains the same $\{[Mo_3S_7]Br\}$ structural motif.[11]

Crystal Structures of $(ET)_3[Mo_3S_7Br_6]_2\cdot CH_2Br_2$ (1) and $(ET)_2[Mo_3S_7Br_6]\cdot 1.1CH_2Br_2$ (2). Compounds **1** and **2** crystallize in the triclinic $P\bar{1}$ space group, and they share several structural features regarding the packing of the organic donor molecules. The asymmetric unit in **1** contains one $[Mo_3S_7Br_6]^{2-}$ dianion and one ET molecule on general positions, labeled as ET_A, and a second ET molecule (ET_B) on a inversion center in agreement with a $(ET_A)_2(ET_B)[Mo_3S_7Br_6]_2$ formulation. On the other hand, the asymmetric unit in **2** with one cluster dianion and two independent ET molecules, namely ET_A and ET_B, in general positions results in a phase with formula $(ET_A)(ET_B)[Mo_3S_7Br_6]$. Highly disordered dibromomethane molecules are also present in both structures.

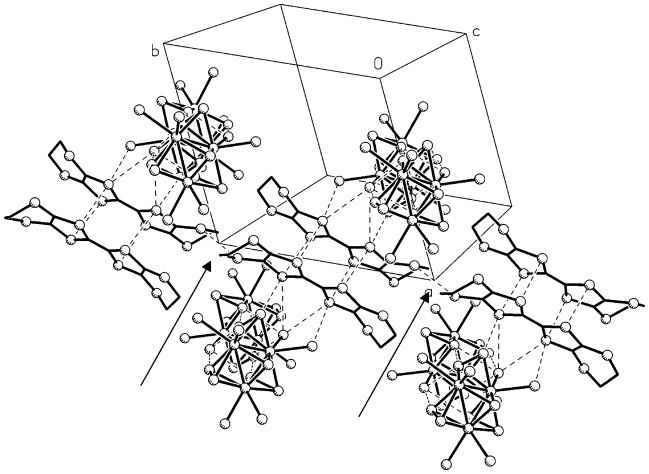

Figure 2. View across the *ab* plane showing the alternating ET_A organic and inorganic layers in $(ET)_2[Mo_3S_7Br_6]\cdot 1.1CH_2Br_2$ (**2**) applicable also to **1**. The contacts marked with arrows differs in both salts being 4.33 and 3.24 Å for compounds **1** and **2**, respectively.

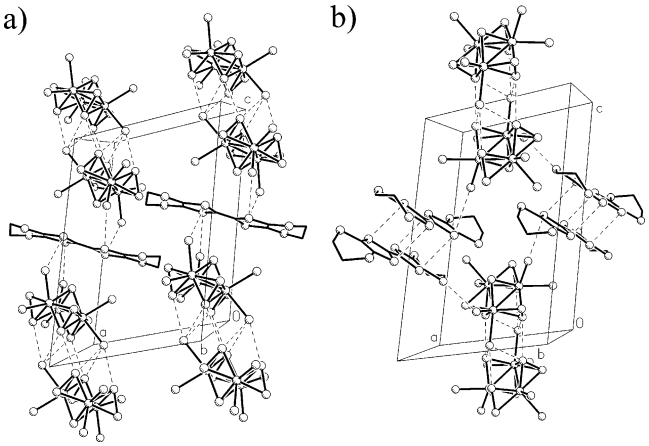

Figure 3. View along the *c* axis showing the identical arrangement between the $[Mo_3S_7Br_6]^{2-}$ cluster anions and the ET_B molecules in (a) compound **1** and (b) compound **2**.

Figure 2 shows the arrangement between the cluster aggregate and the cation labeled as ET_A for compound **2**, but it is also applicable to phase **1**. In both compounds the packing of ET_A consists of dimerized crystallographically equivalent ET_A molecules related by an inversion center with four short face-to-face S···S contacts (below the van der Waals 3.6 Å distance) which results in the formation of layers of organic dimers parallel to the *bc* plane. In compound **2**, the ET_A dimers are further connected through additional side-to-side S···S contacts of 3.24 Å between the sulfur atoms in the outer six-member ring of one dimer with that of the neighbor dimer. The corresponding distance in **1** is considerably longer (4.33 Å) as shown in Figure 2. The packing of the ET_A dimers in **1** and **2** is quite unusual with the long axis of the molecules almost parallel to the cluster layer. A similar arrangement has been described for $(ET)_2[Re_2(NCS)_{10}]\cdot C_6H_5CN$.[36]

The ET_B/cluster packing in compound **1** is represented in Figure 3 together with that of compound **2**, for comparative purposes. The ET_B molecules in **1** connect $\{[Mo_3S_7Br_6]_2\}$

(35) Mori, T.; Wang, P.; Imaeda, K.; Enoki, T.; Inokuchi, H. *Solid State Commun.* **1987**, *64*, 733.

(36) Kepert, C. J.; Kurmoo, M.; Day, P. *Inorg. Chem.* **1997**, *36*, 1128.

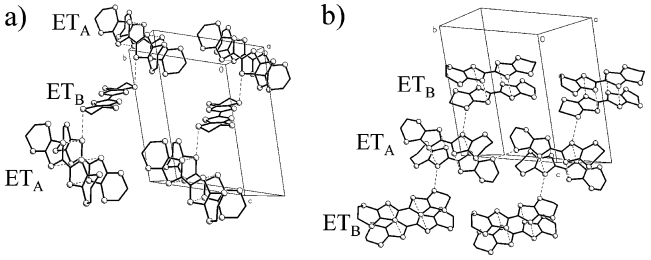

Figure 4. View of the tridimensional and bidimensional whole arrangement of both ET_A and ET_B donor molecules in (a) compound **1** and (b) compound **2**.

dimers through short S···Br (3.31−3.34 Å) contacts to produce alternate $\{[Mo_3S_7Br_6]_2\}-ET_B-\{[Mo_3S_7Br_6]_2\}-ET_B$ ribbons along the *c* axes.

In phase **2**, the ET_B molecules form dimers in a way similar to that described for the ET_A organic units and also connect the $\{[Mo_3S_7Br_6]_2\}$ inorganic dimers to produce alternate $\{[Mo_3S_7Br_6]_2\}-ET_B:ET_B-\{[Mo_3S_7Br_6]_2\}-ET_B:ET_B$ ribbons along the *c* axes. The ET_B dimers in structure **2** roughly occupy the same position as the single ET_B molecules in **1**; however, the cluster ribbon in the unit cell of **2** is shifted along the *a* direction with respect to that of **1** to favor S···S and S···Br contacts between anionic and cationic layers. As a result, differences arise with regard to the relative orientation between the ET_A and ET_B molecules in both structures as shown in Figure 4. The angle defined by the inner plane TTF framework is 110.5 and 18.1° for compounds **1** and **2**, respectively.

The interactions that govern the whole packing involve short contacts between the cluster and solvent bromine atoms with the cluster and the ET sulfur atoms. As a consequence, this packing arrangement arises not from the mismatch of cation and anion layer periodicities but from the S···S and S···Br interactions between cationic and anionic layers.

Donor ion bond lengths are often used to assign oxidation states in charge-transfer salts of ET. From crystallographic data reported above and using the known correlation between the intramolecular C−S and central C═C bond lengths,[37] we can roughly estimate that all the donor molecules in compounds **1** and **2** except the ET_B molecules in **1** are completely ionized (1+) whereas this analysis on the ET_B type donor molecule in this latter compound with a estimated charge value of $Q = (2.3 \pm 0.8)+$ suggests the presence of a ET dication.

Crystal Structures of $(ET)_3\{[Mo_3S_7Br_6]Br\}\cdot 0.5DCE$ (3). Compound **3** crystallizes in the triclinic space group $P\bar{1}$, with the asymmetric unit containing one $[Mo_3S_7Br_6]^{2-}$ anion and one bromine atom forming a trianionic $\{[Mo_3S_7Br_6]Br\}$ aggregate and three independent ET organic molecules (ET_A, ET_B, and ET_C) plus highly disordered DCE molecules. Two of the three crystallographically independent ET cations (ET_B and ET_C) are parallel forming ET_B-ET_C dimers through four short S···S (3.45−3.65 Å) contacts while the other donor molecule ET_A dimerizes with a crystallographically equivalent ET_A molecule related by an inversion center. Within the overall packing of this salt, the arrangement of the ET_A dimers with regard to the inorganic $\{[Mo_3S_7Br_6]Br\}$ aggregate is similar to that represented in Figure 2 for compounds **1** and **2** but replacing the $\{[Mo_3S_7Br_6]_2\}^{4-}$ anion by the $\{[Mo_3S_7Br_6]Br\}^{3-}$ anion. The two remaining organic donor molecules ET_B and ET_C, which form the ET_B-ET_C dimers, produce stepped layers along the *b* axes where each step of the ladder is made by two connected dimers through short S···S (3.54−3.66 Å) contacts. The ET_A dimers are located between these layers and oriented perpendicular to them to give a three-dimensional unique arrangement of ET molecules as shown in Figure 5.

Bond distances found in the three donor molecules in **3** are typical of the fully oxidized (1+) radical cation in good agreement with the compound stoichiometry. The charge of these donor molecules has been confirmed by spectroscopic techniques, and the discussion will be presented in the next section.

Crystal Structures of $(ET)((n\text{-}Bu_4)N)[Mo_3S_7Br_6]$ (4) and $(ET)(Ph_4P)[Mo_3S_7Br_6]\cdot 0.5CH_3CN$ (5). Both salts crystallize in the triclinic space group $P\bar{1}$ containing one $[Mo_3S_7Br_6]^{2-}$ dianion, one independent ET_A organic molecule, the corresponding cation, and disordered solvent molecules. The packing of the cluster:donor system in these two salts is analogous to that represented in Figure 2 for compound **2** and also found in structures **1** and **3**, except that the organic layer in compound **4** runs along the $1\bar{1}0$ direction instead of the *b* axes. The S···S side-to-side short contacts connecting the organic dimers along this directions are 3.23 and 3.19 Å for compounds **4** and **5**, respectively. Figure 6 shows the packing for these two phases including the bulky noninteracting cations.

Both salts form alternate cationic layers where the bulky cation comes quite close to the organic donor layer making these systems very attractive as multicomponent materials. We believe that it would be reasonable to try the incorporation of magnetic and/or active NLO bulky cations with tetrabutylammonium-related topologies as an attempt to combine different properties within the same material. Experiments in that direction are currently in progress in our laboratory.

Again, the bond length analysis also suggests completely ionized donor molecules as observed for **1**−**3**. Nevertheless, the large standard deviations in the considered bond distances for compounds **1**−**5** (typically 0.02 and 0.025 for the C−S and C═C bond lengths, respectively) preclude any definitive assignment. To obtain precise information on this point, we have carried out NIR−vis, IR, and Raman measurements; the results are presented in the following section.

Electronic and Vibrational Spectroscopies. In all the NIR−vis spectra a weak band centered at 11 000−12 000 cm^{-1} (the so-called B band) is observed, corresponding to electron transfers between donor molecules with an integer charge[38] while the absence of the so-called A band in the 3000 cm^{-1} region is indicative of the lack of a mixed-valence

(37) Guinonneau, P.; Kepert, C. J.; Bravic, G.; Chasseau, D.; Truter, M. R.; Kurmoo, M.; Day, P. *Synth. Met.* **1997**, *86*, 1973.

(38) Torrance, J. B.; Scott, B. A.; Welber, F. B.; Kaufman, F. B.; Seiden, P. E. *Phy. Rev. B* **1979**, *19*, 730.

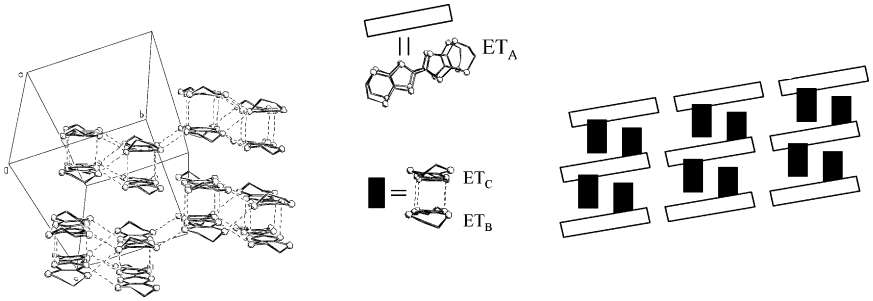

Figure 5. Schematic view of the organic part arrangement for compound **3**. ET_A-type molecules are not included in the ORTEP projection for clarity.

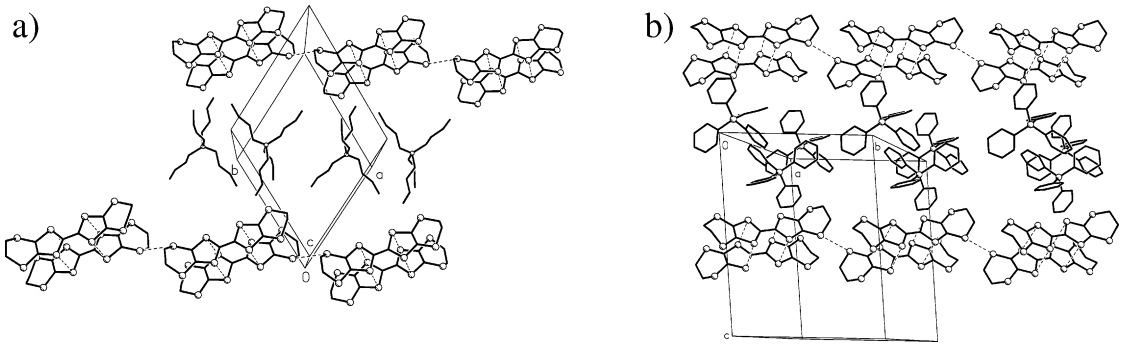

Figure 6. (a) View across the *ab* plane showing the alternating organic layers in (ET)((*n*-Bu_4)N)[$Mo_3S_7Br_6$] (**4**) and (b) view across the *bc* plane showing the alternating organic layers in (ET)(Ph_4P)[$Mo_3S_7Br_6$] (**5**). In both structures the tetranionic clusters have been omitted for clarity.

state in the organic network. These results are consistent with the charge estimated for the donor ET from X-ray analysis and IR and Raman spectroscopies (see below). Two additional bands are observed at 20 000 and 25 000 cm^{-1} which are identical with those observed in the NIR−vis spectra of pure dianionic cluster ((n-Bu_4)N)$_2$[$Mo_3S_7Br_6$] indicating the absence of electronic interaction between the organic and inorganic sublattices in compounds **1**−**5**.

The five radical salts share common features in the IR spectra with a group of bands in the 1400−1450 cm^{-1} region which can be assigned to the vibrational modes associated with the antisymmetric ring C═C stretching. These frequency values are comparable to those obtained for the totally ionized ETBr and ETI_3 salts.[39] The typical bands of the [(*n*-Bu_4)N]$^+$ cation for compound **4** and of the [Ph_4P]$^+$ cation for **5** are also observed. In all salts the $S_{ec}-S_{ax}$ and Mo−μ_2-S IR frequencies appear in the 400−580 cm^{-1} region as commonly reported for this Mo_3S_7 cluster unit.[40]

Raman spectra of the charge-transfer salts are known to reveal essential information on the oxidation state of the donor ET molecules. The vibrational frequencies of the C═C and C−S bonds in this donor molecule are sensitive probes for the oxidation state of the molecule. When electrons are removed from the HOMO, which has bonding characteristics with respect to the C═C bond, the C═C vibration frequencies decrease. Since the HOMO has antibonding characteristics with respect to the C−S bonds, the effect of oxidation is strengthening of the C−S bonds and increase of the C−S frequencies. The Raman spectra for compound **1**−**5** show strong bands in the 1350−1550 cm^{-1} range that can be readily assigned to the totally symmetric Raman-active modes named as $\nu_2(A_g)$ and $\nu_3(A_g)$ according to Kozlov's notation.[39] The symbol in parentheses refers to the mode symmetry assuming a D_{2h} point group for the free ET molecule. These two modes, ν_2 and ν_3, are associated with the two C═C double bonds of the outer six-membered rings and the central C═C double bond, respectively. The charge *Q* can be determined from the linear empirical relationship between the wavenumber and the degree of ionicity.[41,42] This estimation is displayed in Table 3. The resulting charge on the ET molecules within salts **1**−**5** is in excellent agreement with that determined from the X-ray structural analysis, C═C and C−S bond length analysis, and NIR−vis spectra.

Table 3. Charge Distribution in Salts **1**−**5** Derived from the Raman-Active ν_2 and ν_3 A_g Modes[a]

	ν_2 (cm^{-1})	ν_3 (cm^{-1})	Q
$(ET)_3[Mo_3S_7Br_6]_2\cdot CH_2Br_2$ (**1**)	1449	1407	1.12
	1307	1347	2.23
$(ET)_2[Mo_3S_7Br_6]\cdot 1.1CH_2Br_2$ (**2**)	1455	1406	1.05
$(ET)_3\{[Mo_3S_7Br_6]Br\}\cdot 0.5DCE$ (**3**)	1450	1404	1.11
(ET)((*n*-Bu_4)N)[$Mo_3S_7Br_6$] (**4**)	1448	1414	1.06
(ET)(Ph_4P)[$Mo_3S_7Br_6$]$\cdot 0.5CH_3CN$ (**5**)	1451	1400	1.12

[a] ν_2 and ν_3 are associated with the C═C double bonds in the two outer six-membered rings and the central C═C double bond, respectively.

Electrical Properties. The electrical conductivity measurements were performed on single crystals for the whole series. If one pays attention to the collective properties of these phases, owing to the integer oxidation state of all these

(39) Kozlov, M. E.; Pokhodnia, K. I.; Yurchenko, A. A. *Spectrochim. Acta* **1989**, *45A*, 447.
(40) Fedin, V. P.; Kolesov, B. A.; Mironov, Y. V.; Fedorov, V. Y. *Polyhedron* **1989**, *8*, 2419.
(41) Swietlik, R.; Garrigou-Lagrange, C.; Sourisseau, C.; Pages, G.; Delhaès, P. *J. Mater. Chem.* **1992**, *2*, 857.
(42) Hau-Wang, H.; Ferraro, J. R.; Williams, J. M.; Geiser, U.; Schlueter, A. J. *J. Chem. Soc., Chem. Commun.* **1994**, 1893.
(43) Triki, S.; Ouhalab, L.; Halet, J. F.; Peña, O.; Grandjean, D.; Garrigou-Lagrange, C.; Delhaès, P. *J. Chem. Soc., Dalton Trans.* **1992**, 1217.

salts, an insulator or low value of conductivity is expected. Compounds **2** and **4** showed a semiconductor behavior with room-temperature conductivities of 4 and 0.07 $S \cdot cm^{-1}$ and thermal activation energies of 27 and 150 meV, respectively, while compounds **1**, **3**, and **5** resulted to be insulators.

Conclusions

The electrochemical oxidation of the donor ET molecule in the presence of the triangular anionic cluster $[Mo_3S_7Br_6]^{2-}$ has given rise to a new family of radical salts formulated as $(ET)_3[Mo_3S_7Br_6]_2 \cdot CH_2Br_2$ (**1**), $(ET)_2[Mo_3S_7Br_6] \cdot 1.1CH_2Br_2$ (**2**), $(ET)_3\{[Mo_3S_7Br_6]Br\} \cdot 0.5DCE$ (**3**), $(ET)((n\text{-}Bu_4)N)[Mo_3S_7Br_6]$ (**4**), and $(ET)(Ph_4P)[Mo_3S_7Br_6] \cdot 0.5CH_3CN$ (**5**). Although these salts have different stoichiometries and different solid-state structures, all of them share an identical inorganic−organic motif (shown in Figure 2). This characteristic motif is formed by alternating layers of inorganic clusters and ET dimerized units oriented almost parallel to the inorganic layer. Hybrid salts **4** and **5** are made of three different components (cluster:donor:cation), where the bulky cations incorporated are $[(n\text{-}Bu_4)N]^+$ and $[Ph_4P]^+$. The bond distance analysis together with the spectroscopic properties suggests that the ET molecules in these salts are in the +1 (or +2 in the case of ET_B for compound **1**) oxidation state. These integer values of charge agree with the low room-temperature conductivities or the insulator character found for these salts.

Acknowledgment. Financial support from the Ministry of Science and Technology of Spain (Grants BQU2002-00313 and MAT2001- 3507) and from Generalitat Valenciana (Grants IIARCO/2004/159 and IIARCO/2004/161) is acknowledged. We also thank the Servei Central D'Instrumentació Cientifica (SCIC) of the University Jaume I for providing us with the X-ray facilities.

Supporting Information Available: X-ray crystallographic files in CIF format, ORTEP representations of the asymmetric units showing the atom-numbering scheme, and Raman and NIR−vis spectra for compounds **1**−**5**. This material is available free of charge via the Internet at http://pubs.acs.org.

IC0488379